



Granules Reduction in Landscape SAR image based on Deep Denoising and CNN

B. Ramya Banu¹, I.Mounika², I. Navya Reethika³, K.A.S.S.Mounika⁴, S.Saraswathi⁵

Assistant professor, Dept. of ECE, Pragati Engineering College, Surampalem, Andhra Pradesh, India¹

B.Tech Student, Dept. of ECE, Pragati Engineering College, Surampalem, Andhra Pradesh, India^{2,3,4,5}

ABSTRACT: In day-to-day life, the researchers mainly depend on satellite images based on SAR to estimate the conditions on Earth. But while observing these images the features of the image can't be recognized properly because of small granules of noise called Speckle noise. To reduce this we use "Change detection based on deep de-noising and CNN". The Synthetic Aperture Radar (SAR) is used to produce the images that are useful for identifying specific regions on earth. The Convolution Neural Network (CNN) and Deep de-noising are the techniques used in this project to reduce speckle noise, the SAR image is taken as input image which is later de-noised by using the de-noising filter. The deep de-noising model is used to estimate the noise component by training the system and produce a clean image. The image is classified into changed and unchanged area by using the Convolution Neural Network (CNN).

KEYWORDS: Synthetic Aperture Radar, Change Detection, Deep de-noising, Convolution Neural Network (CNN)

I. INTRODUCTION

Synthetic-aperture radar (SAR) is a form of radar image that is used to construct 2D or 3D images reconstructions of objects on the earth, such as landscapes. SAR uses the movement of the radar antenna over a target region to obtain finer spatial resolution than conventional beam-scanning radars. SAR image is captured from moving radar antenna over a target landscape to provide finer spatial resolution than conventional beam-scanning radars. To create a SAR image, successive pulses of radio waves are transmitted to a landscape scene, and the echo of each pulse is received and recorded. Generally if the SAR image aperture is larger than the image resolution will be higher with comparatively physical antennas.

SAR can produce a high-resolution remote sensing image, independent of flight altitude and weather as SAR can choose frequencies to avoid weather-caused signal attenuation. SAR can take images in both day and night as illumination is provided by the SAR.

SAR images have many applications in remote sensing and mapping of surfaces of the Earth and other planets. Applications of SAR involve topography, oceanography, glaciology, geology and forestry, including forest height, biomass, deforestation. Volcano and earthquake monitoring use dissimilar interferometry. SAR can also be used for monitoring civil infrastructure stability such as bridges. SAR is helpful in environment monitoring such as oil spills, flooding, urban growth, global change and military surveillance; involve strategic policy and tactical assessment. SAR can be performed as inverse SAR by observing a moving target above a substantial time with a stationary antenna.

Change Detection has become the major tool in remote sensing research. Change Detection techniques improves the detection performance and stability of SAR images. It can be used in various applications like land cover monitoring, disaster evaluation, resource management, etc.

Convolution Neural Network (CNN) is a class of deep neural network technique. It is applied to analyze visual images. Convolution Neural Networks are used for image classification, segmentation, object detection and drug discovery. It takes an input image, process it and classify it under given categories. The main advantage of CNN is that it can automatically detect the important features without any human supervision.

II. LITERATURE REVIEW

Ulander, L.M.H., Lundberg, M., Pierson [1], Change detection using the frequency of ultra-wideband synthetic aperture radar (SAR) images in the low end of the Very High Frequency band is shown to give excellent performance for detection of vehicle-sized objects in forest concealment. Two algorithms of different change detection are discussed and their performance evaluated. These algorithms are based on similar statistical hypothesis testing, but differ in operations. one operates on complex values(coherent change detection) whereas the other uses magnitude



value (incoherent change detection) of image data. The data were collected during a change detection experiment with captured vehicles in boreal forests. Algorithm results show that coherent change detection using complex values gives better experimental values using full spatial resolution of the images, than the incoherent change detection gives better performance when spatial averaging (2 resolution cells) is included.

Martino, G.D., Iodice, A., Riccio, D [2], presents a complete framework to support the monitoring of natural and man-made disasters by means of synthetic aperture radar (SAR) images. The fractal geometry is the most appropriate mathematical tool in describing the abnormality of a natural observed scene, by means of few effective and dependable parameters. Therefore, fractal concepts can be used to model and find geometrical changes that occurred in areas affected by disasters. A framework which developed includes an algorithm used to extract fractal parameters from a 2D signal using fractal interpolation, and a SAR raw-signal simulator. The combined use of these tools gives an innovative instrument for disaster monitoring applications.

Cao, X., Xiong, T., Jiao, L[4] In order to reduce the subsequent computation burden and storage requirement, band selection has been widely adopted to reduce the dimensionality of hyperspectral images, and the current methods mainly consist of the supervised and the unsupervised. Even though these supervised methods have better performance, those unsupervised methods dominate the band selection field. In this paper, based on the unique properties of hyperspectral images, The algorithm proposed is a very simple but effective supervised band selection algorithm based on the local spatial instrument information of the hyperspectral image and wrapper method. By taking both the data of labeled and unlabeled pixels of the hyperspectral image, the proposed algorithm consistently outsmart the classical wrapper method.

III. EXISTING METHOD

DE-CONVOLUTION

De-convolution, also called deblurring method, It is a computational method that treats the image as an estimate of the true specimen intensity and using an expression for the point spread function performs the inverse of the imaging process to obtain an improved estimate of the image intensity. It is used as a valuable tool that can be used for improving image quality without requiring complicated calculations of the real-time image acquisition and processing systems.

Problem Formulation:

Based on the first order Born approximation, the RF image is assumed to follow a 2D convolution model as below

$$r = Hx + n$$

Where $r \in \mathbb{R}^N$ represents hereby an RF image, i.e. the observation from the acquisition device in a general case $H \in \mathbb{R}^{N \times N}$ is a Block Circulant with Circulant Block (BCCB) matrix related to the 2D point spread function (PSF) of the system and $x \in \mathbb{R}^N$ represents the lexicographically ordered Tissue Reflectivity Function (TRF).

The objective of the de-convolution is to recover x from r . It is not an easy task because

- It is an ill-posed inverse problem and consequently requires proper incorporation of prior knowledge about the TRF x into the restoration process,
- The PSF is usually unknown. The methods assuming the PSF known are categorized as non-blind de-convolution, in opposition to blind de-convolution where the PSF is jointly estimated with x . In the next subsection, we will first assume the PSF known and discuss about the regularizations and corresponding existing non-blind de-convolution algorithms.

REGULARIZATION AND RECOVERY ALGORITHMS:

The previously mentioned target work in (2) can be separated into two sub-issues by the rotating minimization (AM)- based calculation, see, e.g. The main sub-issue, going for evaluating an a and x for a settled h at k th emphasis, can be composed as:

$$(x^{k+1}, a^{k+1}) = \underset{x \in \mathbb{R}^N, a \in \mathbb{R}^N}{\operatorname{argmin}} \|a\|_1 + \alpha P(x) + \frac{1}{2\mu} \|y - \Phi \Psi a\|_2^2 \quad \text{s.t.} \quad H^k x = \Psi a$$

The second sub-problem concerns the estimation of h for fixed a and x :

$$h^{k+1} = \underset{h \in \mathbb{R}^s}{\operatorname{argmin}} \gamma \|h\|_2^2 \quad \text{s.t.} \quad X^{k+1} P h = \Psi a^{k+1}$$



Where $X^{(k+1)} \in \mathbb{R}^{N \times N}$ is a Block Circulant with Circulant Block (BCCB) framework with an indistinguishable structure from H . Its circulant portion is $x^{(k+1)} \in \mathbb{R}^N$. $P \in \mathbb{R}^{(N \times s)}$ is a basic structure lattice mapping the s coefficients of the PSF part h to a N length vector so that

$$[Hx]^{(k+1)} = X^{(k+1)} Ph$$

The obliged issue above can be unraveled by reformulating it as an unconstrained one, subsequently turning into a regularized slightest square issue. Its expository arrangement has been given in

Where $L_s \in \mathbb{R}^s$ is a personality framework, we see that as opposed to transforming a $N \times N$ lattice, we therefore just need to manage the reversal of a $s \times s$ grid.

DAZE DE-CONVOLUTION

For daze deconvolution, the PSF is evaluated from the picture or picture set, enabling the deconvolution to be performed. Specialists have been considering blind deconvolution strategies for a very long while, and have moved toward the issue from various headings.

The majority of the work on daze deconvolution began in mid-1970s. Daze deconvolution is utilized as a part of galactic imaging and therapeutic imaging.

Daze deconvolution can be performed iteratively, whereby every emphasis enhances the estimation of the PSF and the scene, or non-iteratively, where one use of the calculation, in light of outside data, removes the PSF. Iterative strategies incorporate most extreme a posteriori estimation and desire boost calculations. A decent gauge of the PSF is useful for snappier joining yet a bit much.

In this subsection, the current visually impaired de-convolution in which the PSF should be obscure, which is clearly the case in most useful circumstances. Up until now, two sorts of visually impaired de-convolution techniques have been regularly connected to the two fields of general and ultrasound imaging the first is known as from the earlier obscure distinguishing proof strategies in which the PSF is recognized independently from the watched picture and later utilized as a part of blend with one of the non-dazzle de-convolution calculations as portrayed over, the second is called joint ID techniques which evaluate the picture and the PSF at the same time.

A PRIORI BLUR IDENTIFICATION METHODS

In this category, the PSF H and the TRF x are estimated separately and sequentially. Since the x -estimation part has been introduced in the previous subsection, here we only focus on the H -estimation part. One class of algorithms is the parametric ones which explicitly model the PSF with a stochastic or deterministic model. The other class is the nonparametric algorithms. In the proposed high-order spectra (HOS) based approach is shown to be less sensitive to measurement noises. Being non-iterative, it offers some computational advantages and has been used for both axial and lateral de-convolution of RF images.

All the research works, including the prior assumptions made for TRF, the PSF estimation, the non blind de-convolution algorithms and the blind de-convolution, have made it possible to enhance the quality of US images in a post-processing stage.

ALTERNATING DIRECTION METHOD OF MULTIPLIERS (ADMM)

The alternating direction method of multipliers (ADMM) is an algorithm that used to solve convex optimization problems by breaking them into smaller pieces, each of which are then easier to handle. It has recently found many applications in a number of areas.

ADMM has been widely used, in recent years, to solve high dimensional problems in signal and image processing, due to its ability to yield high-quality solutions in a computationally efficient way, in many practical situations. In its original formulation, ADMM can be used to solve problems of the form

$$\underset{u}{\text{minimize}} \quad f(u) + \psi(Ku) \quad (4)$$

where both f and ψ are closed, proper convex, possibly non smooth functions (see Appendix A for details). In comparison with some other primal-dual methods, in the context of image deconvolution, ADMM uses an extra set of variables and involves a matrix inversion. These characteristics, however, apparently are the ones that allow it to remain quite competitive relative to more recent primal-dual methods.



We will use the blurring model of Eq. (4). The noise n will be assumed to be Gaussian. We will use a maximum-a-posteriori (MAP) formulation, and consequently, the datafitting term of our objective function will be given by

$$f(x, z) = \frac{1}{2} \left\| \begin{bmatrix} y \\ z \end{bmatrix} - Hx \right\|^2 \dots (5)$$

with $H = P\tilde{T}$ and $x \in X$, where X is some given convex subset of \mathbb{R}^{k+d} . The problem to be solved will be expressed as

$$\underset{x, z}{\text{minimize}} \quad f(x, z) + \phi(Dx), \tag{6}$$

Where, ($D \in \mathbb{R}^{l \times (k+d)}$) is a matrix that extracts a linear representation of the estimated image, such as edges, l is the number of components of that representation, and $\phi(Dx)$ is a regularize that promotes some desirable characteristic of images, such as sharp edges.

By considering the use of ADMM in its standard form to solve problem (6). The resulting method will not be very efficient, because it will involve a step that is computationally heavy, but it will be useful to motivate the method that proposed in this paper, and to analyse some of its properties. The proposed method, which avoids the above-mentioned computational inefficiency through the use of a partial ADMM. The limitations in the existing methods are Less reduction in noise, The procedure is complex and Results are not accurate.

IV. PROPOSED METHOD

Overview of the proposed method

Change difference (CD) problem can be formulated as a binary classification issue, that is, assigning a label $l = \{0, 1\}$ to each pixel of DL. ‘0’ and ‘1’ are the labels of unchanged and changed pixels, respectively. The main steps of the proposed method are as follows:

- (i) Train the deep denoising model with huge number of simulated SAR images patches.
- (ii) Denoise original SAR image pair with the trained model.
- (iii) Perform CD based on CNN classifier with the denoised SAR image pair.

The proposed method consists of noise reduction in the SAR imaging. Then after denoising the change in the structure is detected. All the two process is done using the deep learning technique. The block diagram of proposed method is given below:

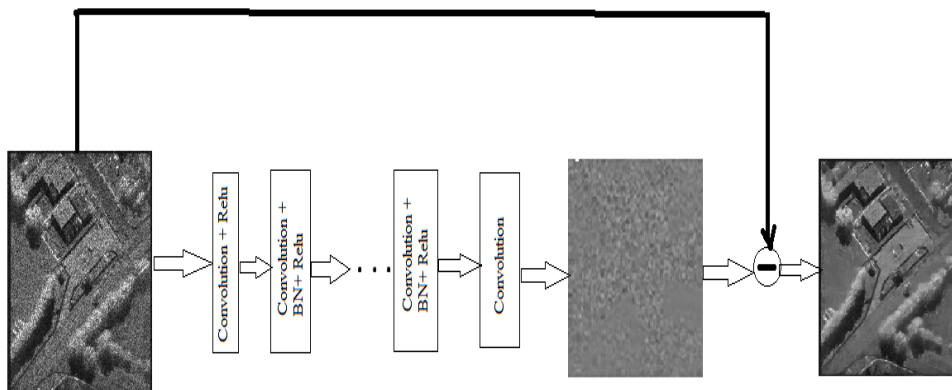


Fig 1: Block diagram of proposed method



CONVOLUTIONAL NEURAL NETWORKS

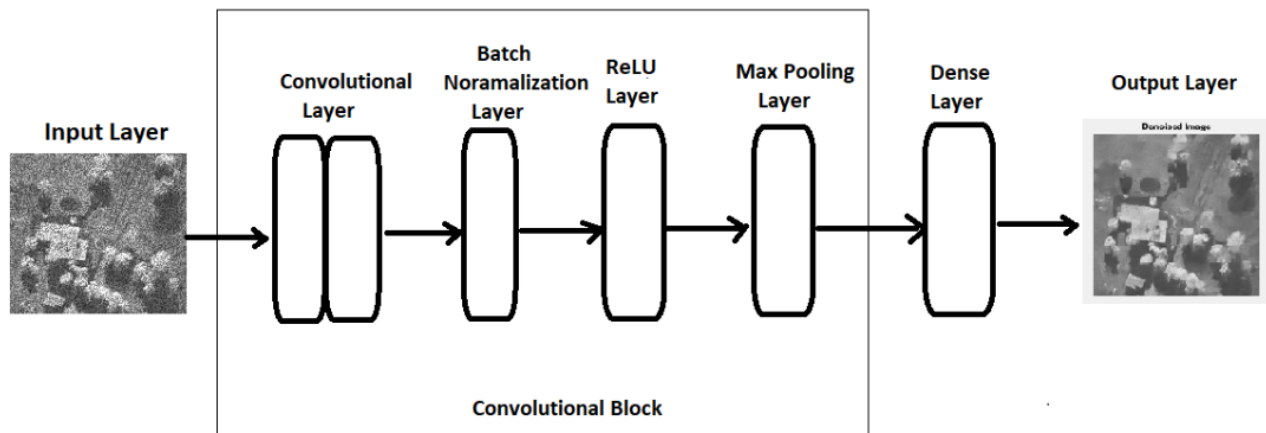


Fig 2: Convolutional Block diagram

Convolution Layer: The convolution layer is the main portion of building block of the CNN. It carries the main portion of the neural network's computational load. This layer performs a dot product between two set of matrices, where one matrix is the set of learnable parameters otherwise known as a kernel, and the other matrix is the restricted portion of the selected field. The kernel is spatially smaller than an image, but is more in-depth. This means that, if the image is composed of three (RGB) color channels, the kernel height and width will be small, but the depth extends up to all three channels. During the forward pass, the kernel move smoothly across the height and width of the image producing the image representation of that selective region. This produces a 2D representation of the image known as an activation map that gives the clear view of the kernel at each spatial position of the image. The sliding size of the kernel in the represented region is called a stride.

Batch Normalization Layer: The next layer in the convolutional neural networks is the batch normalization layer. In this layer each input channel is normalized across a mini-batch which improves the training rate of convolutional neural network and the sensitivity of system is reduced.

ReLU Layer: The Rectified Linear Unit (ReLU) layer is the next layer in the Convolutional Neural Network. This layer acts as an activation unit in the CNN and performs the threshold operation to each element of the input where any value less than zero is said to be zero. It is mathematically defined as $y = \max(0, x)$.

Pooling Layer: The pooling layer replaces the output of the network at certain locations by deriving a summary statistic of the nearby outputs. This helps in reducing the spatial size of the represented image, which decreases the required amount of computation and weights. The pooling operation is processed on every slice of the representation individually. There are several pooling functions such as the average of the rectangular neighborhood, L2 norm of the rectangular neighborhood, and a weighted average based on the distance from the central pixel. However, the most popular process is max pooling, which reports the maximum output from the neighborhood.

Fully Connected Layer: Neurons in this layer have full connectivity with all neurons in the preceding and succeeding layer as in regular FCNN. That is why it can be computed using a regular method by a matrix multiplication followed by a bias effect. The Fully Connected layer helps map the representation between the input and the output.

CNN FOR GRANULES REDUCTION USING CHANGE DETECTION CLASSIFICATION

The internal operation of CNN is shown below

- Start with an input image
- applies many different filters to it to reduce the noise using batch normalization
- applies a ReLU function to increase non-linearity
- applies a pooling layer to each feature map
- Flattens the pooled images into one long vector image.
- Inputs the entire vector into a fully connected artificial neural network.



- Processes the features through the network. The final fully connected layer provides the “voting” of the classes that gives highly accurate results.
- Trains through forward propagation and back propagation for many, many epochs. This repeats until we have a well-defined neural network with trained weights and feature detectors.

Procedure:

At the very beginning of this process, an input image is broken down into pixels.

For a black and white image, those pixels are interpreted as a 2D array (for example, 2x2 pixels). Every pixel has a value between 0 and 255. (Zero is completely black and 255 is completely white. The greyscale exists between those numbers.) Based on that information, the computer can begin to work on the data.

For a color image, this is a 3-Dimensional array with a blue layer, a green layer, and a red layer. Each one of those color has its own value between 0 and 255. The colour can be found by combining the values in each of the three layers.

V. FILTERING METHODS

To remove the noise from an image we use different types of filtering techniques which are used in batch normalization layer. Some of those techniques are given below.

Mean Filtering: Mean filter, or average filter is windowed filter of linear class, that smoothes image. The filter works as low-pass filter. The basic idea behind filter is that for any element of the image take an average across its neighborhood. A mean filter operate on an image take out short noise such as uniform noise and Gaussian type noise from the image at the cost of blurring the image. The arithmetic mean filter is defined as the average of all pixels within a selected region of an image. Pixels that are included in the averaging operation are specified by a mask. The larger the filtering mask becomes most of the part blurring becomes and less high spatial frequency detail that remains in the image.

Median Filtering: A median filter is a nonlinear filter used to remove noise from an image. It is mainly used for removing impulsive type noise from a signal. There are a number of variations of this filter, and a two-dimensional variant is often used in images to remove speckle noise. Median filtering is mostly used in digital image processing because, under certain conditions, it preserves edges while removing noise. This filtering is easy to implement and as it is less sensitive than mean filtering the noise is removed effectively.

Gaussian filtering: Gaussian filtering is a technique which is used to blur the image and remove noise and detail. In one dimension, the Gaussian function is:

$$G(x) = \frac{1}{\sqrt{2\pi\sigma^2}} e^{-\frac{x^2}{2\sigma^2}}$$

Where ‘ σ ’ is the standard deviation of the expression. The distribution expression is assumed to have a mean of zero.

Wiener filtering: The Wiener filtering perform an optimal tradeoff between inverse filtering and noise smoothing. It removes the additive noise and reverse the blurring. The Wiener filtering is best in terms of the mean square error. In other words, it minimizes the total mean square error in the process of inverse filtering and noise smoothing. The Wiener filtering is a linear approximation of the original image.

VI. RESULT AND DISCUSSION**EXPERIMENTAL IMAGE SETS**

Here, training process was conducted using images from three different IQA databases, namely CSIQ [9], LIVE2006 and VCL@FER. Those databases contain respectively 30, 29 and 23 reference images. Each of the databases contain following distortions: blur, additive noise, JPEG compression and JPEG2000 compression.

In this work, speckle noise is treated as additive noise formulated with avoiding logarithm data transformation. With the deep denoising model, estimate noise n and remove it from original image. The visual effect of our denoising method is shown in Fig 3. For a visual comparison, the result of classical despeckling method is listed in comparison of other filtering methods . It is easy to see that the denoised results of SAR are over smoothed. The above results demonstrate that the denoising of SAR images with deep model is feasible.

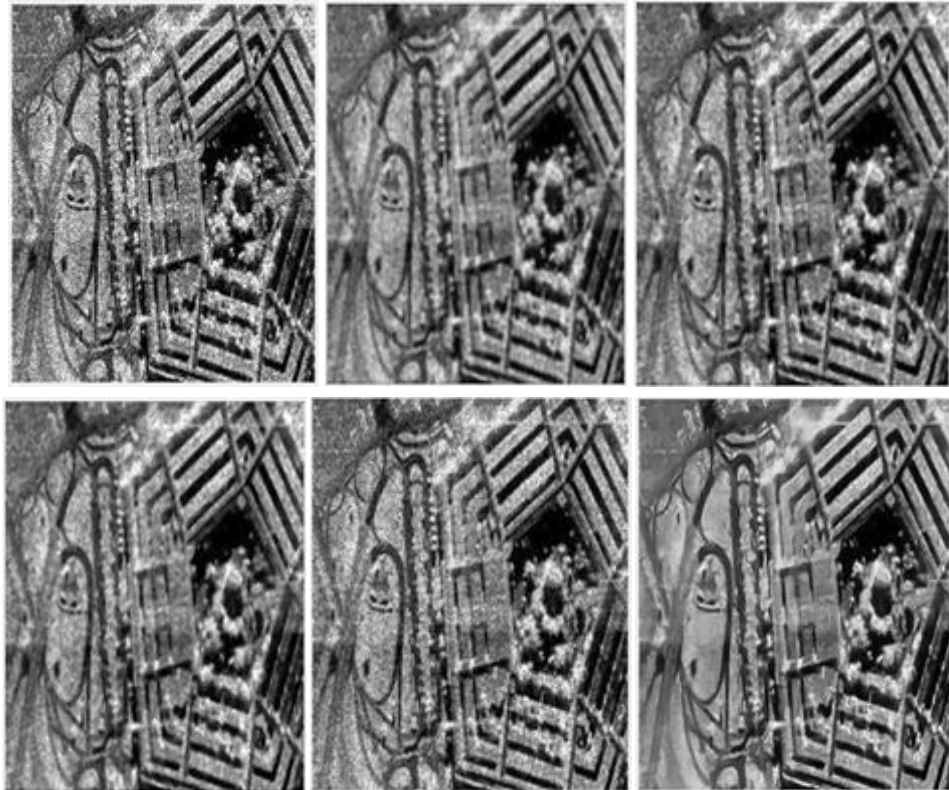


Fig 3. CSIQ [9] sample dataset

(a) Image 1 acquired in August 2019, (b) Denoised image by Mean filtering, (c) Denoised image by Median filtering, (d) Denoised image by Gaussian filtering, (e) Denoised image by Weiner filtering, (f) Denoised image by deep model

PERFORMANCE COMPARISON OF DIFFERENT METHODS

The performance comparison by using different filtering methods for one of the inputs is given below. Though the PSNR and SNR values of some filtering techniques is more for some techniques compared to proposed method, the post filtering characteristics will be good for the proposed method than those techniques.

METHOD	PSNR	SNR	MSE	MAE	SSIM
Mean filtering	20.6029	12.2015	76.4506	9.3069	0.4589
Median filtering	20.4038	11.9354	73.6707	9.3212	0.4658
Gaussian filtering	21.7872	12.5098	40.4200	3.9908	0.9155
Weiner filtering	20.8482	14.5180	71.9128	7.3381	0.6146
Proposed Method	22.5401	15.4417	79.8720	9.6258	0.9269

Table 1: Performance comparison of different noise filtering models

COMPARISON OF DETECTION RESULTS ON THE DIFFERENT DATASET

The experimental results are specified based on different filtering methods, Peak Signal to Noise Ratio (PSNR), Structural Similarity Index(SSIM) and Mean Squared Error(MSE) values. The accurate values shows the proposed deep model is robust to noise and detect quite accurate shape of the changed areas.

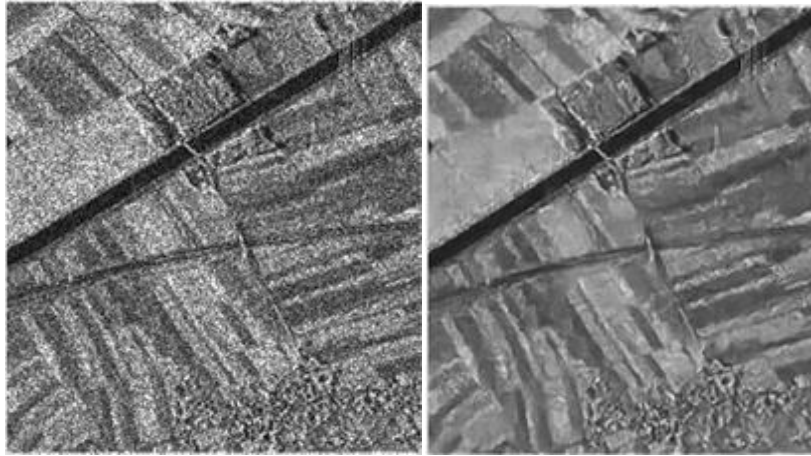


Fig. 4 CSIQ [9]sample dataset-1 (a) Noised image (b) Denoised image

METHOD	PSNR	SNR	MSE	MAE	SSIM
Mean filtering	21.0973	11.1978	78.3206	6.1249	0.4325
Median filtering	19.4128	12.0789	72.1239	6.3982	0.4376
Gaussian filtering	23.7802	15.5098	39.6542	3.1248	0.7158
Weiner filtering	22.8472	14.0098	71.6547	7.1235	0.6347
Proposed Method	27.7872	16.5098	79.4200	7.9908	0.9155

Table 2: Performance comparison of different noise filtering models

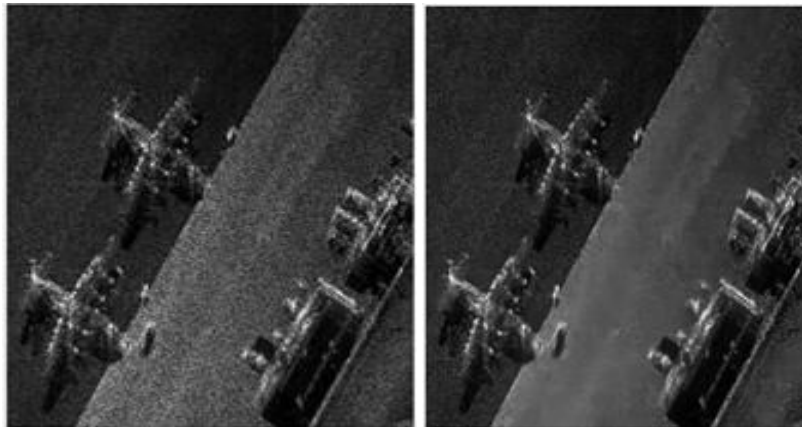


Fig. 5 LIVE2006 sample dataset-2 (a) Noised image (b) Denoised image

METHOD	PSNR	SNR	MSE	MAE	SSIM
Mean filtering	19.0029	11.3016	77.4506	8.2069	0.4679
Median filtering	21.1238	11.9354	73.6707	9.3212	0.4658
Gaussian filtering	20.1246	18.5128	39.4231	3.1208	0.9234
Weiner filtering	21.8764	14.5180	71.9128	7.3381	0.6146
Proposed Method	23.6783	15.7653	72.9821	7.9658	0.7261

Table 3: Performance comparison of different noise filtering models

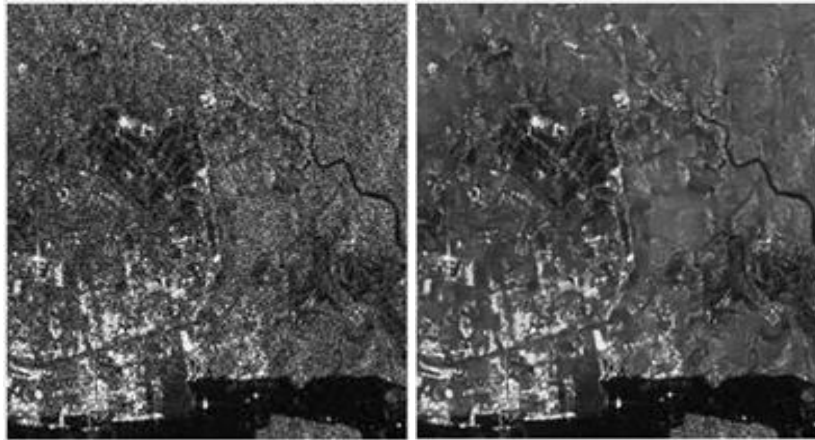


Fig. 6 VCL@FER sample dataset-3 (a) Noised image (b) Denoised image

METHOD	PSNR	SNR	MSE	MAE	SSIM
Mean filtering	20.6029	12.2015	78.4506	9.3069	0.4589
Median filtering	20.0008	11.9354	73.6707	9.3212	0.4658
Gaussian filtering	27.7872	19.5098	40.4200	3.9908	0.9155
Weiner filtering	22.8482	14.5180	71.9128	7.3381	0.6146
Proposed Method	22.5401	14.4417	70.8720	7.3258	0.6269

Table 4: Performance comparison of different noise filtering models

VII CONCLUSION

A high-quality Difference Image(DI) is crucial to the success of the Change Detection(CD). In this paper, the deep de-noising model and CNN model are combined to construct a SAR CD algorithm. Deep denoising is used to keep useful information and suppress noise simultaneously. After denoising, DI is generated by the clean de-noised image pair. To learn the discriminative features from DI, three layers of CNN model are used for feature learning tool. At last, DI are classified by a softmax classifier. The proposed method first embraces deep denoising and deep feature learning into SAR CD and obtains a satisfactory result. In reality, SAR images are very different with optical images. In our future work, we will apply our denoising model to facilitate real-world applications, including image retrieval, image understanding and classification.

REFERENCES

- [1] Ulander, L.M.H., Lundberg, M., Pierson, W., *et al.*: ‘Change detection for low-frequency SAR ground surveillance’, *IEE Proc., Radar Sonar Navig.*, 2005, **152**, (6), pp. 413–420
- [2] Martino, G.D., Iodice, A., Riccio, D., *et al.*: ‘A novel approach for disaster monitoring: fractal models and tools’, *IEEE Trans. Geosci. Remote Sens.*, 2007, **45**, (6), pp. 1559–1570.
- [3] Sim, K.M.: ‘Grid commerce, market-driven g-negotiation, and grid resource management’, *IEEE Trans. Syst. Man Cybern. B (Cybern.)*, 2006, **36**, (6), pp.1381–1394.
- [4] Bruzzone, L., Prieto, D.F.: ‘An adaptive semiparametric and context-based approach to unsupervised change detection in multitemporal remote-sensing images’, *IEEE Trans. Image Proc. A Publ. IEEE Signal Proc. Soc.*, 2002, **11**, (4), pp. 452–466.
- [5] Cao, X., Xiong, T., Jiao, L.: ‘Supervised band selection using local spatial information for hyperspectral image’, *IEEE Geosci. Remote Sens. Lett.*, 2016, **13**, (3), pp. 329–333.
- [6] Dabov, K., Foi, A., Egiazarian, K.: ‘Image denoising with block-matching and 3d filtering’. Proc. of SPIE – The Int. Society for Optical Engineering, 2006, vol. 6064, pp. 354–365.
- [7] Cao, X., Wei, C., Han, J., *et al.*: ‘Hyperspectral band selection using improved classification map’, *IEEE Geosci. Remote Sens. Lett.*, 2017, **PP**, (99), pp. 1–5